Journal of Theoretical Biology 580 (2024) 111719

Contents lists available at ScienceDirect

Journal of Theoretical Biology

journal homepage: www.elsevier.com/locate/yjtbi

Antigenic cooperation in viral populations: Transformation of functions of intra-host viral variants☆

Leonid Bunimovich [a], Athulya Ram [a,b,*], Pavel Skums [c]

[a] School of Mathematics, Georgia Institute of Technology, Atlanta, 30332, GA, USA
[b] Interdisciplinary Graduate Program in Quantitative Biosciences, Georgia Institute of Technology, Atlanta, 30332, GA, USA
[c] Department of Computer Science and Engineering, University of Connecticut, Storrs, 06269, CT, USA

ARTICLE INFO

Keywords:
Local immunodeficiency
Cross-immunoreactivity
Persistent viruses
Altruistic viruses
Hepatitis c

ABSTRACT

In this paper, we study intra-host viral adaptation by antigenic cooperation - a mechanism of immune escape that serves as an alternative to the standard mechanism of escape by continuous genomic diversification and allows to explain a number of experimental observations associated with the establishment of chronic infections by highly mutable viruses. Within this mechanism, the topology of a cross-immunoreactivity network forces intra-host viral variants to specialize for complementary roles and adapt to the host's immune response as a quasi-social ecosystem. Here we study dynamical changes in immune adaptation caused by evolutionary and epidemiological events. First, we show that the emergence of a viral variant with altered antigenic features may result in a rapid re-arrangement of the viral ecosystem and a change in the roles played by existing viral variants. In particular, it may push the population under immune escape by genomic diversification towards the stable state of adaptation by antigenic cooperation. Next, we study the effect of a viral transmission between two chronically infected hosts, which results in the merging of two intra-host viral populations in the state of stable immune-adapted equilibrium. In this case, we also describe how the newly formed viral population adapts to the host's environment by changing the functions of its members. The results are obtained analytically for minimal cross-immunoreactivity networks and numerically for larger populations.

1. Introduction

RNA viruses such as HIV, Hepatitis C (HCV), Zika, Influenza A, and SARS-CoV-2 are characterized by extremely high evolutionary rates (Drake and Holland, 1999). As a result, each infected host or a community of infected individuals carries a heterogeneous population of genetically related viral variants (Domingo et al., 2012) that exist as an ecosystem, with the dominant selection pressure caused by hosts' immune systems (Rhee et al., 2007). Until recently, the predominant model of viral evolution was the immune escape via continuous accumulation of genetic diversity (Nowak and May, 2000) often described as an "arms race" between virus and hosts. However, several recent experimental discoveries suggest a possibly more complex picture. These discoveries include broad cross-immunoreactivity and antigenic convergence between intra-host viral variants (Campo et al., 2012), a consistent increase in negative selection, and a decrease in population heterogeneity over time (Ramachandran et al., 2011; Campo et al., 2014; Gismondi et al., 2013; Lu et al., 2008; Illingworth et al., 2014), long-term persistence of viral variants (Ramachandran et al., 2011; Palmer et al., 2012, 2014) and complex fluctuations of frequencies of subpopulations over the course of infection (Ramachandran et al., 2011; Gismondi et al., 2013; Palmer et al., 2014; Gray et al., 2012; Raghwani et al., 2016). Given these observations, it is unlikely that the entire viral evolution is driven by a single evolutionary mechanism. It is rather a non-linear process defined by the recurring presentation of a succession of selection challenges specific to different stages of infection or epidemic spread (Baykal et al., 2021). Each stage involves complex mechanisms that viruses share with other domains of life (Domingo-Calap et al., 2019; Baykal et al., 2021).

Many previously studied mathematical models of virus–host immune system interactions (Nowak and May, 2000; Wodarz, 2003; Iwasa et al., 2004) suggest that immune escape is associated with a constant increase in genomic heterogeneity, and does not account for certain experimentally observed phenomena. One of the most intriguing such phenomena of intra-host viral evolution is the transition between the immune escape under

☆ The authors acknowledge the support of Georgia Tech Interdisciplinary Graduate Program in Quantitative Biosciences. Funding: This work was partially supported by the NIH, United States grant R01EB025022 and NSF, United States grant CCF-2047828.

* Corresponding author.
E-mail addresses: leonid.bunimovich@math.gatech.edu (L. Bunimovich), athulya@gatech.edu (A. Ram), pavel.skums@uconn.edu (P. Skums).

https://doi.org/10.1016/j.jtbi.2023.111719
Received 6 April 2023; Received in revised form 10 September 2023; Accepted 20 December 2023
Available online 27 December 2023

positive selection at an early stage of infection and a conditionally stable state under negative selection at the later stage. Several previously published models link this phenomenon with the effects of cross-immunoreactivity. In particular, the studies (Haraguchi and Sasaki, 1997; Gog and Grenfell, 2002) provide explanations of prolonged stasis in immune escape and the coexistence of clusters of intra-host variants within a classical "arms race" paradigm. Other recently published modeling, genomic, and experimental studies suggest that this transition can be caused by the development of specific cooperative interactions among viral variants (Skums et al., 2015a; Shirogane et al., 2013; Domingo-Calap et al., 2019; Baykal et al., 2021) that allow viral populations to adapt to their environment as quasi-social systems (Domingo-Calap et al., 2019).

The ODE model describing interactions between viral antigens and host B cells predicting and describing one possible scenario of such interactions has been proposed and analyzed in our previous studies (Skums et al., 2015a; Bunimovich and Shu, 2019, 2020; Bunimovich et al., 2019). Cross-immunoreactivity network (CRN) plays a central role there. Although cross-immunoreactivity is essential for neutralization, its role is more complex and ambiguous. In particular, it does not always act as a factor of pressure on the virus but rather may serve as a factor facilitating virus survival through the mechanisms of original antigenic sin, heterologous immunity, and antibody-dependent enhancement of viral infectivity (Francis, 1960; Rehermann and Shin, 2005; Parsons et al., 2013; Meyer et al., 2008). The model assumes the presence of CRN with complex topology and takes into account a fundamental biochemical difference between antigenicity (capacity to bind antibodies) and immunogenicity (capacity to elicit antibodies) (Van Regenmortel, 2012; Campo et al., 2012; Freitas et al., 1995; McLean et al., 1997; Tarlinton, 2006; Schwickert et al., 2007; Palmer et al., 2012). As a result, it describes a dynamic fitness landscape where viral variants determine the fitness of other variants through their interactions in CRN. Antigenic cooperation and specialization of viral variants are naturally implied by the model as a way of mitigating the immune pressure on certain antigenic variants at the expense of other variants. The state when the immune neutralization of particular variants is hampered is provisionally called *local immunodeficiency* (Skums et al., 2015a). The structure of CRN determines specific roles for each viral variant in host adaptation and local immunodeficiency emergence. Variants of high in-degrees play an *altruistic* role and improve the fitness of adjacent variants at their own fitness cost by developing a polyspecific antibody response that interferes with the development of specific immune responses against other variants immunoreactive with these antibodies. The latter variants are *selfish* because they gain fitness at the expense of in-hub variants. Thus, the model describes a cooperation between neighbors in CRN which in some aspects resembles altruism through kin selection (Hamilton, 1964), with the relatedness by epitope similarity serving in place of the genetic relatedness. This mechanism allows to explain a number of empirical observations. It is also stable and robust under various realistic conditions (Bunimovich and Shu, 2019).

Notably, the antigenic cooperation model achieves its predictive power by using fewer variables than most of the previously proposed models (Wodarz, 2003; Nowak et al., 1990, 1991; Nowak and May, 1991). The reasons for that is that are (a) the high non-linearity of the model that allows to capture non-linear evolutionary effects; (b) the more delicate exploration of the effects of cross-immunoreactivity via the introduction of CRN with a complex topology as a model parameter, in contrast to mean-field approximation of immune responses utilized by many existing models.

Antigenic cooperation model has been rigorously studied in several prior papers. The original paper (Skums et al., 2015a), besides introducing the model, described the emergence of antigenic cooperation and local immunodeficiency as its inherent properties using both numerical simulations and analytical exploration of its equilibrium solutions. The paper (Bunimovich and Shu, 2019) demonstrated that solutions implying local immunodeficiency can be stable and robust under various realistic conditions for several specific types of cross-immunoreactivity networks. Another paper (Bunimovich and Shu, 2020) studied the role of altruistic viral variants in intra-host adaptation. It demonstrated that without altruistic variants the viral population could maintain only a marginally stable state of local immunodeficiency and a relatively small size.

However, viral populations and, consequently, cross-immunoreactivity networks are not static and are subject to dynamical changes caused by the emergence or introduction of viral variants with altered phenotypes. This fact raises a fundamental question: whether or how changes in CRNs lead to evolutionary transitions and, in particular, what are the effects of such changes on the functions of specific viral variants and on the immune escape of the entire population?

This question is the focus of the present paper. We study dynamical changes in B cell immune adaptation caused by two types of evolutionary and epidemiological events: (a) the emergence of a new viral variant with altered antigenic phenotype and (b) a viral transmission between two chronically infected hosts, which results in the merging of two intra-host viral populations in the state of stable immune-adapted equilibrium. Both phenomena are typical for evolution of the intra-host viral populations and important for understanding the laws of their evolution.

We analyze these processes statically, assuming that the emergence of new antigenic variants occurs in a given state of a virus–host system, and analyzing what will be a new stable state of the system. This new stable state will be (formally) achieved in an infinite time. Then we study this process of transition from an "old" state to the new one dynamically by following the previous evolution of the initial network and then its (future) dynamics after the emergence of new variants.

It turned out that such events may result in a rapid re-arrangement of the viral ecosystem and a change of the roles played by viral variants. In addition, it is rigorously demonstrated that emergent antigenic variants may successfully co-exist with present persistent variants and become persistent itself while keeping the state of stable local immunodeficiency in the CRN. Another, less expected, and potentially more important finding, is that the emergence of new variants may push the population under immune escape by genomic diversification towards the stable state of adaptation by antigenic cooperation. These findings emphasize how phenotypic features of particular viral genomic variants are formed by both their antibody and "quasi-social" environments rather than pre-defined by their genomes. They also highlight challenges in effective vaccine design by demonstrating how the evolutionary trajectories of intra-host viral populations subjected to the introduction of new antigenic variants are affected by the state of pre-existing populations.

The paper is organized as follows. In the next section, we present a basic model of intra-host viral evolution in the presence of a complex cross-immunoreactivity network. Section 3 deals with the transformations that result from the emergence of a new viral variant in the population under a stable state of local immunodeficiency (LI). In Section 4 we analyze the process of the union of two CRNs each having a stable state of LI. All technical computations are presented in the Appendix.

2. Model of evolution of intra-host viral population organized into heterogeneous cross-immunoreactivity network

In this section, we describe the mathematical model of the viral population organized into a heterogeneous cross-immunoreactivity network. The model was introduced in Skums et al. (2015a) and applied to the Hepatitis C virus, but applies to any highly mutable pathogen with a broad spectrum of cross-immunoreactivity. We consider a population of n viral antigenic variants x_i inducing n immune responses r_i in the form of antibodies and memory B-cells. We assume that viral variants form a cross-immunoreactivity network. This network can be represented as a

weighted directed graph $G_{CRN} = (V, E)$, i.e. a graph with a set of vertices V and a set of edges E. Vertices of the graph correspond to viral variants and a pair of vertices u and v are connected by an edge if v-specific antibodies elicited by v as an immunogen interact with an antigen u by binding to the appropriate epitopes with sufficiently high affinity. We incorporate the asymmetry between immune activation and neutralization into the model by considering two weight functions for the edges of G_{CRN}. These functions are described by immune neutralization and immune stimulation matrices $U = (u_{i,j})_{i,j=1}^{n}$ and $V = (v_{i,j})_{i,j=1}^{n}$, where: $0 \le u_{i,j}, v_{i,j} \le 1$; $u_{j,i}$ is a coefficient representing the binding affinity of antibodies r_j with ith variant; and $v_{i,j}$ is a coefficient reflecting the strength of stimulation of antibodies to r_j by ith variant. The immune response r_i against the variant x_i is neutralizing; i.e., $u_{ii} = v_{ii} = 1$.

The resulting viral and antibody population dynamics are described by the following system of ordinary differential equations:

$$\begin{aligned} \dot{x}_i &= f_i x_i - p x_i \sum_{j=1}^{n} u_{ji} r_j, \quad i = 1, \dots, n, \\ \dot{r}_i &= c \sum_{j=1}^{n} x_j \frac{v_{ji} r_i}{\sum_{k=1}^{n} v_{jk} r_k} - b r_i, \quad i = 1, \dots, n. \end{aligned} \tag{1}$$

In this model, a viral variant x_i replicates at the rate f_i and is eliminated by the immune responses r_j at the rates $pu_{ji}r_j$,where p is a constant. An immune responses r_i proliferate at the rate proportional to the concentrations of variants recognized by it weighted by the corresponding immune stimulation coefficients, thus describing the clonal selection. In addition, the proliferation rate associated with the stimulation of the response r_i by the j-the antigenic variant is proportional to the non-linear term $g_{ji} = \frac{v_{ji} r_i}{\sum_{k=1}^{n} v_{jk} r_k}$ representing the probability of stimulation by x_j in the presence of other antigens competing for stimulation by that variant. This model assumption describes another aspect of clonal selection theory — the immunological memory, whereat x_j preferentially stimulates pre-existing immune responses capable of binding to x_j with a relatively high affinity (Nara et al., 2010). Immunological memory provides a rapid secondary immune response to re-infections with the same pathogen, but also results in the original antigenic sin, repertoire freeze, and heterologous immunity (Francis, 1960; Kim et al., 2009; Midgley et al., 2011; Parsons et al., 2013; Rehermann and Shin, 2005). Without stimulation, immune responses r_i decay at the rate b. It should be noted that for a single viral variant or in the absence of cross-immunoreactivity ($U = V = \mathrm{Id}$), the model (1) reduces to the linear immune response model of immune-pathogen interaction that has been considered in prior studies (see Nowak and May (2000)).

Similarly to Skums et al. (2015b), Bunimovich and Shu (2019), here we are mostly interested in the effects of the CRN structure (topology) on the population dynamics. Thus we consider the situation where the immune stimulation and neutralization coefficients are equal to constants α and β, respectively. In this case, we have

$$U = \mathrm{Id} + \beta A^T, V = \mathrm{Id} + \alpha A,$$

where A is the adjacency matrix of the graph G_{CRN}, the $n \times n$ matrix where a_{ij} represents the number of edges from variant j to variant i. In numerical simulations, we assume that $0 < \beta = \alpha^k$, where k is the number of epitopes that should be bound for neutralization.

Note that in the absence of cross-immunoreactivity, the system (1) reduces to the model described in Nowak and May (2000). In that case, equilibrium sizes of populations of viral variants and immune responses are

$$x_i^\circ = \frac{b f_i}{c p}, r_i^\circ = \frac{f_i}{p}, \tag{2}$$

One of the most interesting properties of the system (1) is the emergence of the so-called state of *local immunodeficiency*. It is defined as an equilibrium solution $(\mathbf{x}^*, \mathbf{r}^*)$ such that every viral variant i falls into one of the following 3 categories:

(1) $x_i^* > 0$ and $r_i^* \le r_i^\circ$ (*persistent variants*);
(2) $x_i^* = 0$ and $r_i^* > 0$ (*altruistic variants*);
(3) $x_i^* = r_i^* = 0$ (*transient variants*).

Transient variants are being eliminated by the host's immune system as they emerge, and thus are subject to the standard immune escape by continuous diversification mechanism. The relations between persistent and altruistic variants are more interesting, as they describe a different mechanism of immune escape by antigenic cooperation. Under this mechanism, persistent variants survive without eliciting any specific immune responses (the state of "local immunodeficiency" with respect to these variants, where the immune system effectively "does not see" them). This is achieved via the agency of altruistic variants that do not survive but support the continuous existence of persistent variants. The roles of viral variants in this scheme are defined by their position in the CRN, with altruistic variants usually (but not always) being network hubs, and persistent variants being adjacent to them. Qualitatively, the mechanism can be described as follows. Under the model (1), if the viral variant x_i is adjacent to an altruistic variant x_j, then the immune response r_i competes for activation with the immune response r_j. Since the latter response is broadly cross-immunoreactive and being stimulated by many variants, even after the elimination of x_i ($x_i = 0$), it is preserved and readily outcompetes the former response, thus preventing it from development ($r_j = 0$). At the same time, r_j-antibodies may lack sufficiently high affinity to neutralize x_i, which leads to its persistence ($x_j > 0$). One can consider these interactions as a form of cooperation between altruistic and persistent variants, where the former lose their fitness by significantly contributing to the fitness of the latter.

The state of local immunodeficiency, when exists, is usually stable and robust, as was confirmed both analytically and numerically (Skums et al., 2015a; Bunimovich and Shu, 2019, 2020).

3. Emergence of a new viral variant

This section deals with the situation when a new variant is added to a cross-immunoreactivity network. We found that as a result, the roles of viral variants may change in different ways.

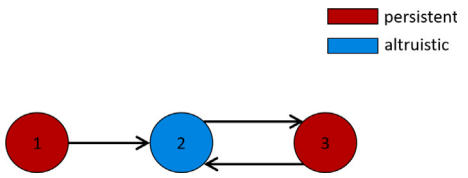

Fig. 1. Stable configuration of the branch-cycle network. Node categories are highlighted in different colors. There are three viral variants in this network. Immune response against variant 2 is stimulated by both variants 1 and 3. Variant 2 stimulates the immune response against variant 3.

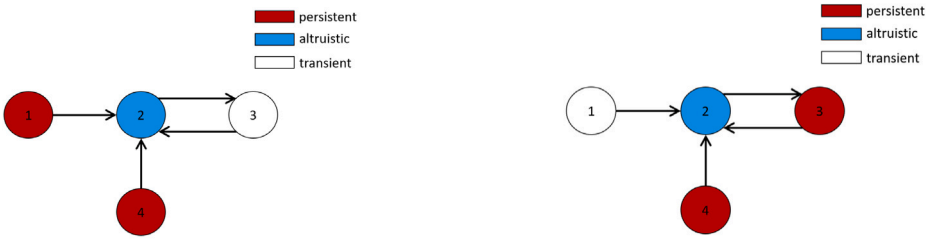

Fig. 2. Stable states where the emerging viral variant 4 becomes persistent in a branch-cycle network. A new variant (4) has been added to the network in Fig. 1. Immune response against variant 2 is stimulated by variants 1, 3, and 4. Variant 2 stimulates the immune response against variant 3.

3.1. Adding a new viral variant to a minimal branch-cycle network

A branch-cycle network is one of just the two smallest CR networks (Bunimovich and Shu, 2019, 2020) which can exhibit the property of a stable and robust local immunodeficiency. The network and the roles of viral variants in the corresponding solution (that is derived and described in Bunimovich and Shu (2019, 2020)) are depicted in Fig. 1. We analyzed all possible additions of a new node to this network and the resulting equilibrium solutions.

The most notable finding is the existence of solutions where the introduction of a new node changes the functions of preexisting variants. All such stable solutions are shown in Fig. 2; in all cases, the change occurs when a new variant (node 4) is linked to the altruistic variant of the previous configuration. Other cases (where the newly emerged viruses are connected to a pre-existing persistent virus) are detailed in Appendix A.3.

The fixed point shown in Fig. 2(a) corresponds to the following solution:

$$x_1^* = \frac{b(\beta f_1 + (\alpha-\beta)f_4)}{\beta c p}, \quad x_2^* = 0, \quad x_3^* = 0, \quad x_4^* = \frac{b f_4(1-\alpha)}{\beta c p}$$
$$r_1^* = \frac{f_1 - f_4}{p}, \quad r_2^* = \frac{f_4}{\beta p}, \quad r_3^* = 0, \quad r_4^* = 0$$

This fixed point is stable under the conditions $\alpha > \frac{1}{2}, f_1 > f_4, f_4 > f_3$, and $f_4 > \beta f_2$ (see Appendix A.1)

The second fixed point shown in Fig. 2(b) corresponds to

$$x_1 = 0, \quad x_2 = 0, \quad x_3 = \frac{b(\beta f_3 + (\alpha-\beta)f_4)}{\beta c p}, \quad x_4 = \frac{b f_4(1-\alpha)}{\beta c p}$$
$$r_1 = 0, \quad r_2 = \frac{f_4}{\beta p}, \quad r_3 = \frac{f_3 - f_4}{p}, \quad r_4 = 0$$

This fixed point is stable if $\alpha > \frac{1}{2}, f_4 > f_1, f_3 > f_4$, and $f_4 > \beta f_2$ (see Appendix A.1)

Changes described by these two solutions are structurally similar. In both cases newly added variant becomes persistent, while the previously persistent variant is eliminated by the immune system and the altruistic variant retains its role. A necessary condition for the stability of such qualitative changes in viruses functions is that the replication rate of an emergent variant is greater than that of the preexisting persistent variant.

Notably, in both cases, the change occurs in the variant not adjacent to the newly added variant. It demonstrates how network-mediated interactions between viral variants propagate along the cross-immunoreactivity networks and thus go beyond direct interactions described in Section 2. In this particular case, we observe a natural selection acting on potentially persistent variants supported by the same altruistic variant, with the variant of the lower fitness being eliminated and replaced by the newly emerged variant.

The fact that the newly emerging variant is cross-immunoreactive as an antigen with the immune response against a pre-existing altruistic variant is essential. Indeed, when variant 4 is cross-immunoreactive with variants 1 or 3, then it either becomes transient while the roles of pre-existing variants are unchanged, or the dynamics of the CR network becomes unstable, i.e. it does not have a stable and robust state of local immunodeficiency.

3.2. Adding a new viral variant to a minimal symmetric network

A symmetric network (Bunimovich and Shu, 2020) is another instance of the two smallest CR networks that can exhibit stable state of local immunodeficiency (Fig. 3).

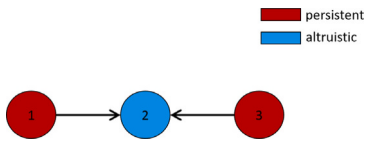

Fig. 3. Symmetric minimal network. There are three viral variants in this network. Immune response against variant 2 is stimulated by variants 1 and 3.

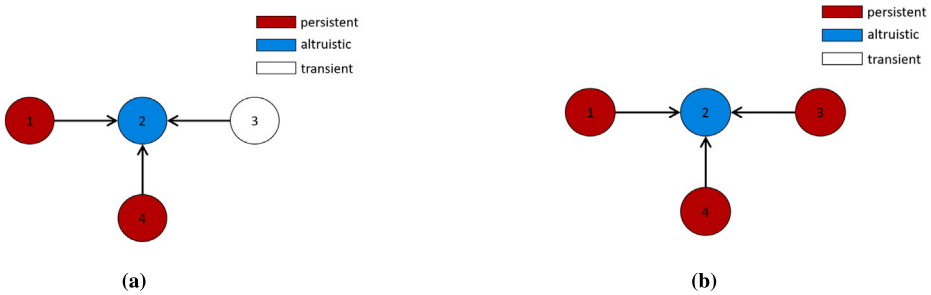

Fig. 4. Stable states where the new viral variant connected to the altruistic variant becomes persistent in a symmetric network. A new variant (4) has been added to the network in Fig. 3. Immune response against variant 2 is stimulated by variants 1, 3, and 4.

It was proven in Bunimovich and Shu (2020) that a stable state of LI exists in this network if $f_3 > f_1$, with the fixed point corresponding to

$$x_1 = \frac{bf_1}{cp\beta}(1-\alpha), \qquad x_2 = 0, \qquad x_3 = \frac{b}{cp\beta}(\alpha f_1 + \beta(f_3 - f_1))$$
$$r_1 = 0, \qquad r_2 = \frac{f_1}{p\beta}, \qquad r_3 = \frac{f_3 - f_1}{p}$$

As this network is symmetric, there is a similar fixed point with the switched solutions for variants 1 and 3; that solution is stable under the condition $f_1 > f_3$.

When a new viral variant that is cross-immunoreactive with the pre-existing altruistic variant is added to this network, the functions of the viruses could change in two possible ways. The fixed point shown in Fig. 4(a) is described as follows:

$$x_1 = \frac{b(\beta f_1 + (\alpha-\beta)f_4)}{\beta cp}, \quad x_2 = 0, \quad x_3 = 0, \quad x_4 = \frac{bf_4(1-\alpha)}{\beta cp}$$
$$r_1 = \frac{f_1 - f_4}{p}, \quad r_2 = \frac{f_4}{\beta p}, \quad r_3 = 0, \quad r_4 = 0$$

The stability conditions of this fixed point are $\alpha > \frac{1}{2}, f_1 > f_4, f_4 > f_3$, and $f_4 > \beta f_2$ (see Appendix A.2). Naturally, there exists a symmetric solution, with the variant 1 rather than variant 3 being transient.

Another fixed point (Fig. 4(b)) is given via the following relations

$$x_1 = \frac{b(\beta f_1 + (\alpha-\beta)f_4)}{\beta cp}, \quad x_2 = 0, \quad x_3 = \frac{b(\beta f_3 + (\alpha-\beta)f_4)}{\beta cp}, \quad x_4 = \frac{bf_4(1-2\alpha)}{\beta cp}$$
$$r_1 = \frac{f_1 - f_4}{p}, \quad r_2 = \frac{f_4}{\beta p}, \quad r_3 = \frac{f_3 - f_4}{p}, \quad r_4 = 0$$

Conditions of stability of this fixed point are $\frac{1}{3} < \alpha < \frac{1}{2}, f_1 > f_4, f_3 > f_4$, and $f_4 > \beta f_2$. (see Appendix A.2)

In both instances, the newly added variant becomes persistent only when it is attached to the altruistic variant. This seems to be a natural result from the perspective of the local immunodeficiency mechanism (see Section 2). In other aspects, however, the instances describe somewhat different evolutionary phenomena. In the solution depicted in Fig. 4(a), the newly emerged variant substitutes the previously persistent variant by virtue of having a higher replication rate, thus providing an example of natural selection action under the local immunodeficiency mechanism. In contrast, for the solution from Fig. 4(b), the emerging variant has a lower replication rate than the existing persistent variants. Thus, it neither eliminates these variants nor eliminates itself, but rather co-exists with them. In this environment, previous persistent variants continue to exist in the same role, although under higher immune pressures and lower population sizes.

Furthermore, the second solution reveals the previously unnoticed phenomenon, where a dynamical change in the topology of the cross-immunoreactivity network leads to the emergence of a stable LI in the population when it previously did not exist. Indeed, the symmetric minimal network in Fig. 3 has a stable LI only under the condition $\alpha > \frac{1}{2}$. The stable state of LI exhibited by the solution in Fig. 4(b) exists under the condition $\frac{1}{3} < \alpha < \frac{1}{2}$, which means that with these values of α the initial 3-network did not have a stable LI, but acquired it after the addition of a new variant to the network.

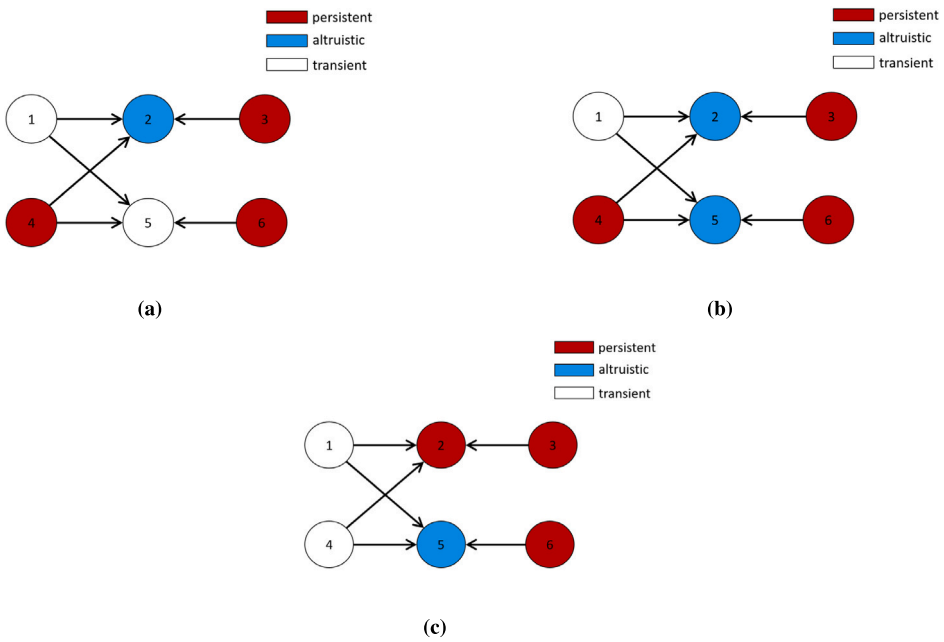

Fig. 5. Examples of transformation of function after joining minimal networks. There are essentially six viral variants in all these examples. An arrow from variant i to variant j indicates that variant i stimulates the immune response against variant j.

4. Merging of two cross-immunoreactivity networks

In this section, we describe the changes in the system states caused by a viral transmission between a pair of chronically infected hosts. We assume that both hosts are infected for a sufficiently long period of time for their intra-host populations to develop a state of stable immune-adapted equilibrium. Transmissions of HCV are usually associated with a relatively wide bottleneck, with multiple transmission/founder (T/F) variants being transmitted from the donor to the recipient (Campo et al., 2017). As a result, a subgraph of a CR network of a donor formed by the T/F variants is merged with the pre-existing CR network of a recipient. In what follows, we present three cases when the merging of two minimal symmetric CR networks leads to the state of stable local immunodeficiency. All other analyzed cases of network merging destroy the stability of this state.

Fig. 5(a) depicts a solution for a 6-vertex network obtained by joining two symmetric 3-vertex networks induced by vertices 1–3 and 4–6, respectively. The fixed point corresponding to 5(a) is given by the following relations

$$x_1 = 0, \qquad r_1 = 0$$
$$x_2 = 0, \qquad r_2 = \frac{f_4}{\beta p}$$
$$x_3 = \frac{b(\beta f_3 + (\alpha - \beta) f_4)}{\beta c p}, \qquad r_3 = \frac{f_3 - f_4}{p}$$
$$x_4 = \frac{b f_4 (1 - \alpha)}{\beta c p}, \qquad r_4 = 0$$
$$x_5 = 0, \qquad r_5 = 0$$
$$x_6 = \frac{b f_6}{c p}, \qquad r_6 = \frac{f_6}{p}$$

In this solution, previously altruistic variants 5 and previously persistent variant 1 become transient. Once the transient variants are eliminated by the immune system, the cross-immunoreactivity network breaks into two subnetworks, one of which (induced by variants 2,3,4) is isomorphic to a minimal network shown in Fig. 3. The variant 6 is isolated from the remaining variants, effectively evolves in the absence of cross-immunoreactivity and thus converges to the corresponding stable state. Another possibility leading to the stable state of LI is presented in Fig. 5(b): here a single variant (variant 1) is eliminated, i.e. changes its role from persistent to transient. The corresponding fixed point of this network is

$$x_1 = 0, \qquad r_1 = 0$$
$$x_2 = 0, \qquad r_2 = \frac{f_4 - \beta f_5}{\beta p}$$
$$x_3 = \frac{b(\beta f_3 + (\alpha - \beta)(f_4 - \beta f_5))}{\beta c p}, \qquad r_3 = \frac{f_3 - f_4 + \beta f_5}{p}$$
$$x_4 = \frac{b f_4 (1 - \alpha)}{\beta c p}, \qquad r_4 = 0$$

$$x_5 = 0, \qquad r_5 = \frac{f_5}{p}$$
$$x_6 = \frac{b((\alpha-\beta)f_5 + f_6)}{cp}, \qquad r_6 = \frac{f_6 - \beta f_5}{p}$$

Finally, the solution from Fig. 5(c) describes an outcome, when the elimination of 1 and 4 breaks the CR network into two 2-vertex subnetworks reflecting different degrees of local immunodeficiency; both of these states were described in the original publication (Skums et al., 2015a). The corresponding fixed point is

$$x_1 = 0, \qquad r_1 = 0$$
$$x_2 = \frac{bf_2(1-\alpha)}{cp}, \qquad r_2 = \frac{f_2}{p}$$
$$x_3 = \frac{b((\alpha-\beta)f_2 + f_3)}{cp}, \qquad r_3 = \frac{f_3 - \beta f_2}{p}$$
$$x_4 = 0, \qquad r_4 = 0$$
$$x_5 = 0, \qquad r_5 = \frac{f_6}{\beta p}$$
$$x_6 = \frac{bf_6}{\beta cp}, \qquad r_6 = 0$$

For this solution, the subnetwork induced by vertices 2 and 3 exist in the state, when equilibrium values of x_3 and r_3 depend not only on f_3 but also on f_2. It means that the variant 3 achieves a higher population size under lower immune pressure (in comparison with the system without CR) by exploiting the replicative ability the variant 2. The subnetwork formed by variants 5 and 6 expresses a stronger form of the same phenomenon, where the variant 6 exists without any 5-specific immune pressure (i.e. under the strong state of LI) due to the presence of the 5-specific antibodies, whose high concentration is supported entirely by the variant 6 (with r_5 depending only on f_6). The interesting property of the latter subnetwork is that the corresponding subsolution is stable for a positive measure set in the parameter space, when considered within the 6-vertex network; in contrast, it is stable only for $\alpha = 1$, when considered within the 2-vertex network (Skums et al., 2015a).

5. Transformation of functions in evolving networks

In the previous sections, we analyzed the equilibrium solutions describing the asymptotic properties of the system (2). In this section, we discuss the entire dynamics of intra-host viral populations before and after new variants are added to the CRN networks. Since the model (2) is a highly nonlinear dynamical system, which gives no hope of obtaining an analytic solution, the analysis in this section is, by necessity, numerical. In the context of this study, particularly interesting is the speed of transition between different states of the system and the change of viral variant roles in the population's intra-host adaptation, including the elimination of previously persistent variants due to the network expansion.

The results are presented in Fig. 6. Naturally, the dynamics of transformations of the populations from Figs. 6(a) and 6(b) (Fig. 6(a)) are qualitatively similar, which is to be expected given the qualitative similarity of their asymptotic solutions (see Section 3.2). In both cases, the elimination of previously persistent variants (variants 3 and 1, respectively) happens quite quickly. The same is true for the immune response against the altruistic variant 2, which is boosted by the emergence of a new immunogen 4, thus allowing to sustain the adaptation of two persistent variants (1,4 and 3,4, respectively) under the state of local immunodeficiency.

In contrast, the time evolution of populations shown in Figs. 6(c) and 6(d) essentially differ from each other, with the speed of transition of the latter population being significantly more rapid. As above, this difference can be explained by the properties of the corresponding asymptotic solutions. Indeed, the initial state in the first network (Fig. 6(c)) is a stable local immunodeficiency. On the contrary, the initial state in the network in Fig. 6(d) is unstable local immunodeficiency. Therefore it is natural that the transition between stable states goes slower. Furthermore, the higher concentration of the altruistic variants-specific antibodies achieved for the population 6(d) allows to sustain the adaptation of 3 rather than 2 persistent variants.

6. Discussion

In this paper, we study the dynamic and equilibrium properties of a model (Skums et al., 2015a; Bunimovich and Shu, 2019, 2020; Bunimovich et al., 2019) describing the behavior of an intra-host viral population that is organized into cross-immunoreactivity (CR) networks and is under pressure by the host's adaptive immune system in the form of variant-specific B-cells. One of the prominent features of this model is the emergence of the so-called state of local immunodeficiency, i.e. the equilibrium state where the immune neutralization of certain variants is suppressed due to the interactions between pre-existing antigens and antibodies mediated by the CR network. We concentrate on the transitions between the population states caused by dynamic changes in the CR network topology. Specifically, we investigate two events — the introduction of a new antigenic variant to the CR network, and the merging of two CR networks in the state of stable immune-adapted equilibrium, which may occur, for example, from a viral transmission between two chronically infected hosts.

It was shown that with the emergence of a new antigenic variant, there can be a rapid rearrangement in the roles played by the variants. A newly emerged variant can become persistent under the following two conditions: (1) the new antigenic variant is cross-immunoreactive with the antibodies specific to the existing altruistic variant and (2) the newly emerged variant has a higher replication rate than a previously persistent variant. This type of rearrangement is expected when the initial system had stable local immunodeficiency before the emergence of a new variant.

Furthermore, we have shown that the appearance of a novel antigenic variant results in the establishment of a stable local immunodeficiency within a viral population that initially did not exhibit such a condition. This finding diverges from the outcomes of earlier studies, which primarily concentrated on identifying fixed CR networks with a stable local immunodeficiency state. This discovery paves the way for further exploration of CR network dynamics leading to the development of stable LI states.

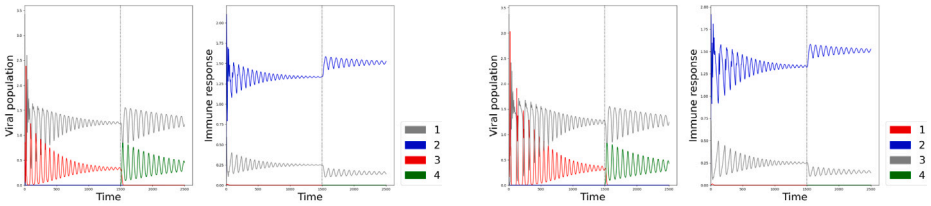

(a) Dynamics of the transformation of function in the network in figure 2a. Parameters used: $f_1 = 2, f_2 = 1, f_3 = 1.5, f_4 = 1.7, c = 1, p = 1, \alpha = 2/3, \beta = 4/9, b = 1$

(b) Dynamics of the transformation of function in the network in figure 2b. Parameters used: $f_1 = 2, f_2 = 1, f_3 = 1.5, f_4 = 1.7, c = 1, p = 1, \alpha = 2/3, \beta = 4/9, b = 1$

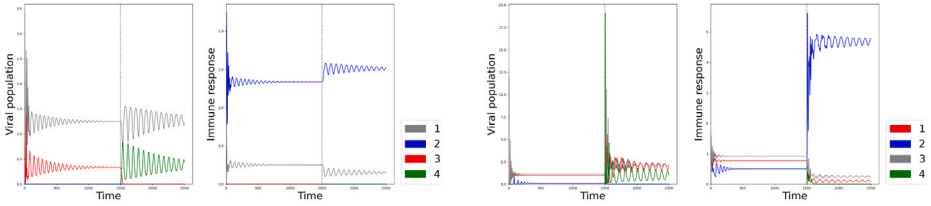

(c) Dynamics of the transformation of function in the network in figure 4a. Parameters used: $f_1 = 2, f_2 = 1, f_3 = 1.5, f_4 = 1.7, c = 1, p = 1, \alpha = 2/3, \beta = 4/9, b = 1$

(d) Dynamics of the transformation of function in the network in figure 4b. Parameters used: $f_1 = 1.7, f_2 = 1, f_3 = 2, f_4 = 1.5, c = 1, p = 1, \alpha = 2/5, \beta = 4/25, b = 1$

Fig. 6. Dynamics of minimal networks before and after the introduction of a new variant. Left figures depict the dynamics of variant population sizes, and right figures — of the variant-specific immune responses. Dotted lines represent moments of time when the new variants are added to CR networks.

Similar transitions have been observed for the merging of CR networks. It was shown in several examples how the roles of antigenic variants in the CR networks are rearranged, how certain variants are eliminated, and how the CR networks can break down into subnetworks with different phenotypes.

In addition to the analytical results of equilibrium states, we also analyze numerically the time-evolution of the dynamics of CR networks before and after the emergence of a new viral variant. We find that the transition between two different stable LI states is slower compared to the transition that creates a stable state of LI.

This study underscores the non-linear nature of intra-host viral evolution, which exhibits extended periods of stability, interrupted by rapid shifts due to the emergence of viral variants with altered antigenic phenotypes. This process can be likened to the concept of punctuated equilibrium in macroevolution. Similar patterns have been noted in other studies (Haraguchi and Sasaki, 1997; Gog and Grenfell, 2002); in the model examined, these patterns result from CRN-mediated interactions. From an epidemiological standpoint, the research highlights the important role of outbreaks and subepidemics in high-risk settings, where transmissions occur frequently between chronically infected or previously exposed hosts. Such environments may promote frequent disturbances in equilibrium, thus increasing the effective rate of viral evolution and increasing the likelihood of emergence of phenotypically altered variants. This underscores the urgent need for targeted community-based public health interventions that focus on testing, containment, and eradication of viral pathogens for such high-risk host subpopulations (Nagot et al., 2023; Organization et al., 2016). Finally, the highlighted equilibrium disruption mechanism provides potential insights for vaccine development. This can be achieved through immunization with carefully chosen or engineered neutralizing epitopes that can thwart the viral population's adaptation to host immunity.

The study certainly has a number of limitations. The analyzed model, though relatively rich, is not comprehensive, and does not account for several immunological phenomena, including T cell immunity and antibody competition for neutralization (in contrast to the competition for activation, as considered by the model (1)). Furthermore, analytical solutions have been studied only for certain small networks, that by no means represent the whole spectrum of possible CRN topologies. Development of more comprehensive models and analytical study of more complex populations are challenging and hopefully will constitute subjects of future studies.

Declaration of competing interest

The authors declare the following financial interests/personal relationships which may be considered as potential competing interests: Leonid Bunimovich, Pavel Skums reports financial support was provided by National Institutes of Health. Pavel Skums reports financial support was provided by National Science Foundation.

Appendix

Computations corresponding to the minimal networks can be found in Bunimovich and Shu (2019) (branch-cycle network, Fig. 1), and Bunimovich and Shu (2020) (symmetric network, Fig. 3).

A.1. Computations for the branch-cycle network with a newly added variant connected to the pre-existing altruistic variant

Fig. 2 depicts two configurations of the branch-cycle network with stable state of local immunodeficiency, where the variant 4 is newly added. The dynamics (1) of this population is described by the following equations

$$\begin{aligned}
\dot{x}_1 &= f_1 x_1 - p x_1 (r_1 + \beta r_2),\\
\dot{x}_2 &= f_2 x2 - p x_2 (r_2 + \beta r_3),\\
\dot{x}_3 &= f_3 x_3 - p x_3 (r_3 + \beta r_2),\\
\dot{x}_4 &= f_4 x_4 - p x_4 (r_4 + \beta r_2),\\
\dot{r}_1 &= c\left(\frac{x_1 r_1}{r_1 + \alpha r_2}\right) - b r_1,\\
\dot{r}_2 &= c\left(\frac{\alpha x_1 r_2}{r_1 + \alpha r_2} + \frac{x_2 r_2}{r_2 + \alpha r_3} + \frac{\alpha x_3 r_2}{r_3 + \alpha r_2} + \frac{\alpha x_4 r_2}{r_4 + \alpha r_2}\right) - b r_2,\\
\dot{r}_3 &= c\left(\frac{\alpha x_2 r_3}{r_2 + \alpha r_3} + \frac{x_3 r_3}{r_3 + \alpha r_2}\right) - b r_3,\\
\dot{r}_4 &= c\left(\frac{x_4 r_4}{r_4 + \alpha r_2}\right) - b r_4.
\end{aligned} \tag{A.1}$$

The Jacobian of the system of (A.1) at the fixed point shown in Fig. 2(a) is:

$$\begin{pmatrix}
0 & 0 & 0 & 0 & -\frac{b(\alpha f_4+\beta f_1-\beta f_4)}{\beta c} & -\frac{b(\alpha f_4+\beta f_1-\beta f_4)}{c} & 0 & 0\\
0 & f_2-\frac{f_4}{\beta} & 0 & 0 & 0 & 0 & 0 & 0\\
0 & 0 & f_3-f_4 & 0 & 0 & 0 & 0 & 0\\
0 & 0 & 0 & 0 & 0 & \frac{b f_4(\alpha-1)}{c} & 0 & \frac{b f_4(\alpha-1)}{\beta c}\\
\frac{\beta c(f_1-f_4)}{\alpha f_4+\beta f_1-\beta f_4} & 0 & 0 & 0 & -\frac{b\beta(f_1-f_4)}{\alpha f_4+\beta f_1-\beta f_4} & -\frac{\alpha b\beta(f_1-f_4)}{\alpha f_4+\beta f_1-\beta f_4} & 0 & 0\\
\frac{\alpha c f_4}{\alpha f_4+\beta f_1-\beta f_4} & c & c & c & -\frac{\alpha b f_4}{\alpha f_4+\beta f_1-\beta f_4} & -\frac{b(\alpha f_4+\beta f_1-\beta f_4-\alpha\beta f_1+\alpha\beta f_4)}{\alpha f_4+\beta f_1-\beta f_4} & 0 & \frac{b(\alpha-1)}{\alpha}\\
0 & 0 & 0 & 0 & 0 & 0 & -b & 0\\
0 & 0 & 0 & 0 & 0 & 0 & 0 & -\frac{b(2\alpha-1)}{\alpha}
\end{pmatrix}$$

We will verify the stability of this fixed point by analyzing the eigenvalues of this system. Recall at first the conditions of stability of the fixed point, which were mentioned earlier in Section 3.1 : $\frac{1}{2} < \alpha < 1, f_1 > f_4, f_4 > f_3$, and $f_4 > \beta f_2$.

With the parameters $f_1 = 2, f_2 = 1, f_3 = 1.5, f_4 = 1.7, c = 1, p = 1, \alpha = 2/3, \beta = 4/9, b = 1$ that satisfy these conditions, the eigenvalues of the system at this fixed point are:

$$\begin{aligned}
\lambda_1 &= -2.8250 & \lambda_2 &= -1.0000\\
\lambda_3 &= -0.5000 & \lambda_4 &= -0.2000\\
\lambda_5 &= -0.4990 + 1.2884i & \lambda_6 &= -0.4990 - 1.2884i\\
\lambda_7 &= -0.0185 + 0.2978i & \lambda_8 &= -0.0185 - 0.2978i
\end{aligned}$$

Hence we can generate a system with the CRN in Fig. 2(a) which has a stable and robust steady state of LI. Thus we present an exact example with the stable state of local immunodeficiency.

The Jacobian of the differential Eqs. (A.1) at the fixed point shown in Fig. 2(b) is:

$$\begin{pmatrix}
f_1-f_4 & 0 & 0 & 0 & 0 & 0 & 0 & 0\\
0 & -\frac{f_4-\beta f_2+\beta^2 f_3-\beta^2 f_4}{\beta} & 0 & 0 & 0 & 0 & 0 & 0\\
0 & 0 & 0 & 0 & 0 & -\frac{b(\alpha f_4+\beta f_3-\beta f_4)}{c} & -\frac{b(\alpha f_4+\beta f_3-\beta f_4)}{\beta c} & 0\\
0 & 0 & 0 & 0 & 0 & \frac{b f_4(\alpha-1)}{c} & 0 & \frac{b f_4(\alpha-1)}{\beta c}\\
0 & 0 & 0 & 0 & -b & 0 & 0 & 0\\
c & \frac{c f_4}{f_4+\alpha\beta f_3-\alpha\beta f_4} & \frac{\alpha c f_4}{\alpha f_4+\beta f_3-\beta f_4} & c & 0 & -\frac{b(\alpha f_4+\beta f_3-\beta f_4-\alpha\beta f_3+\alpha\beta f_4)}{\alpha f_4+\beta f_3-\beta f_4} & -\frac{\alpha b f_4}{\alpha f_4+\beta f_3-\beta f_4} & \frac{b(\alpha-1)}{\alpha}\\
0 & \frac{\alpha\beta c(f_3-f_4)}{f_4+\alpha\beta f_3-\alpha\beta f_4} & \frac{\beta c(f_3-f_4)}{\alpha f_4+\beta f_3-\beta f_4} & 0 & 0 & -\frac{\alpha b\beta(f_3-f_4)}{\alpha f_4+\beta f_3-\beta f_4} & -\frac{b\beta(f_3-f_4)}{\alpha f_4+\beta f_3-\beta f_4} & 0\\
0 & 0 & 0 & 0 & 0 & 0 & 0 & -\frac{b(2\alpha-1)}{\alpha}
\end{pmatrix}$$

We will verify the stability of this fixed point by analyzing the eigenvalues of this system. Recall at first the conditions of stability of the fixed point, which were mentioned earlier in Section 3.1 : $\frac{1}{2} < \alpha < 1, f_4 > f_1, f_3 > f_4$, and $f_4 > \beta f_2$.

With the parameters $f_1 = 2, f_2 = 1, f_3 = 1.5, f_4 = 1.7, c = 1, p = 1, \alpha = 2/3, \beta = 4/9, b = 1$ that satisfy these conditions, the eigenvalues of the system at this fixed point are:

$$\lambda_1 = -2.9583 \qquad \lambda_2 = -1.0000$$
$$\lambda_3 = -0.5000 \qquad \lambda_4 = -0.2000$$
$$\lambda_5 = -0.4990 + 1.2884i \qquad \lambda_6 = -0.4990 - 1.2884i$$
$$\lambda_7 = -0.0185 + 0.2978i \qquad \lambda_8 = -0.0185 - 0.2978i$$

Hence we can generate a system with the CRN in Fig. 2(b) which has a stable and robust steady state of LI.

A.2. Computations for the symmetric network with a newly added variant connected to the pre-existing altruistic variant

Fig. 4 depicts two stable configurations of the branch-cycle network where the variant 4 is newly added.
The dynamics (1) of this population is described by the following equations

$$\begin{aligned}
\dot{x}_1 &= f_1 x_1 - p x_1 (r_1 + \beta r_2),\\
\dot{x}_2 &= f_2 x2 - p x_2 r_2,\\
\dot{x}_3 &= f_3 x_3 - p x_3 (r_3 + \beta r_2),\\
\dot{x}_4 &= f_4 x_4 - p x_4 (r_4 + \beta r_2),\\
\dot{r}_1 &= c\left(\frac{x_1 r_1}{r_1 + \alpha r_2}\right) - b r_1,\\
\dot{r}_2 &= c\left(\frac{\alpha x_1 r_2}{r_1 + \alpha r_2} + x_2 + \frac{\alpha x_3 r_2}{r_3 + \alpha r_2} + \frac{\alpha x_4 r_2}{r_4 + \alpha r_2}\right) - b r_2,\\
\dot{r}_3 &= c\left(\frac{x_3 r_3}{r_3 + \alpha r_2}\right) - b r_3,\\
\dot{r}_4 &= c\left(\frac{x_4 r_4}{r_4 + \alpha r_2}\right) - b r_4.
\end{aligned} \tag{A.2}$$

At the fixed point shown in Fig. 4(a), the Jacobian of the system (A.2) equals

$$\begin{pmatrix}
0 & 0 & 0 & 0 & -\frac{b(\alpha f_4+\beta f_1-\beta f_4)}{\beta c} & -\frac{b(\alpha f_4+\beta f_1-\beta f_4)}{c} & 0 & 0\\
0 & f_2-\frac{f_4}{\beta} & 0 & 0 & 0 & 0 & 0 & 0\\
0 & 0 & f_3-f_4 & 0 & 0 & 0 & 0 & 0\\
0 & 0 & 0 & 0 & 0 & \frac{b f_4(\alpha-1)}{c} & 0 & \frac{b f_4(\alpha-1)}{\beta c}\\
\frac{\beta c(f_1-f_4)}{\alpha f_4+\beta f_1-\beta f_4} & 0 & 0 & 0 & -\frac{b\beta(f_1-f_4)}{\alpha f_4+\beta f_1-\beta f_4} & -\frac{\alpha b\beta(f_1-f_4)}{\alpha f_4+\beta f_1-\beta f_4} & 0 & 0\\
\frac{\alpha c f_4}{\alpha f_4+\beta f_1-\beta f_4} & c & c & c & -\frac{\alpha b f_4}{\alpha f_4+\beta f_1-\beta f_4} & -\frac{b(\alpha f_4+\beta f_1-\beta f_4-\alpha\beta f_1+\alpha\beta f_4)}{\alpha f_4+\beta f_1-\beta f_4} & 0 & \frac{b(\alpha-1)}{\alpha}\\
0 & 0 & 0 & 0 & 0 & 0 & -b & 0\\
0 & 0 & 0 & 0 & 0 & 0 & 0 & -\frac{b(2\alpha-1)}{\alpha}
\end{pmatrix}$$

The conditions of stability of the fixed point are (see the Section 3.1) $\alpha > \frac{1}{2}, f_1 > f_4, f_4 > f_3$, and $f_4 > \beta f_2$.
We will verify the stability of this fixed point by analyzing the eigenvalues of this system. With the parameters $f_1 = 2$, $f_2 = 1$, $f_3 = 1.5$, $f_4 = 1.7$, $c = 1$, $p = 1$, $\alpha = 2/3$, $\beta = 4/9$, $b = 1$ that satisfy these conditions, the eigenvalues of the system at this fixed point are:

$$\lambda_1 = -2.8250 \qquad \lambda_2 = -1.0000$$
$$\lambda_3 = -0.5000 \qquad \lambda_4 = -0.2000$$
$$\lambda_5 = -0.4990 + 1.2884i \qquad \lambda_6 = -0.4990 - 1.2884i$$
$$\lambda_7 = -0.0185 + 0.2978i \qquad \lambda_8 = -0.0185 - 0.2978i$$

Hence we can generate a system with the CRN in Fig. 4(a) which has a stable and robust steady state of LI.
At the fixed point of the network in Fig. 4(b), the Jacobian of the system of Eqs. (A.2) is $J = (XYZ)$ where

$$X = \begin{pmatrix}
0 & 0 & 0 & 0 & -\frac{b(\alpha f_4+\beta f_1-\beta f_4)}{\beta c}\\
0 & f_2-\frac{f_4}{\beta} & 0 & 0 & 0\\
0 & 0 & 0 & 0 & 0\\
0 & 0 & 0 & 0 & 0\\
\frac{\beta c(f_1-f_4)}{\alpha f_4+\beta f_1-\beta f_4} & 0 & 0 & 0 & -\frac{b\beta(f_1-f_4)}{\alpha f_4+\beta f_1-\beta f_4}\\
\frac{\alpha c f_4}{\alpha f_4+\beta f_1-\beta f_4} & c & \frac{\alpha c f_4}{\alpha f_4+\beta f_3-\beta f_4} & c & -\frac{\alpha b f_4}{\alpha f_4+\beta f_1-\beta f_4}\\
0 & 0 & \frac{\beta c(f_3-f_4)}{\alpha f_4+\beta f_3-\beta f_4} & 0 & 0\\
0 & 0 & 0 & 0 & 0
\end{pmatrix},$$

$$Y = \begin{pmatrix} -\frac{b(\alpha f_4+\beta f_1-\beta f_4)}{c} \\ 0 \\ -\frac{b(\alpha f_4+\beta f_3-\beta f_4)}{c} \\ \frac{b f_4(2\alpha-1)}{c} \\ -\frac{\alpha b\beta(f_1-f_4)}{\alpha f_4+\beta f_1-\beta f_4} \\ \left(\frac{1}{(\beta f_1+(\alpha-\beta)f_4)(\beta f_3+(\alpha-\beta)f_4)} (b(\alpha^2 {f_4}^2+\beta^2 {f_4}^2-2\alpha\beta^2 {f_4}^2+2\alpha^2\beta {f_4}^2 \right. \\ -2\alpha\beta {f_4}^2+\beta^2 f_1 f_3-\beta^2 f_1 f_4-\beta^2 f_3 f_4-2\alpha\beta^2 f_1 f_3+ \\ \left. 2\alpha\beta^2 f_1 f_4-\alpha^2\beta f_1 f_4+2\alpha\beta^2 f_3 f_4-\alpha^2\beta f_3 f_4+\alpha\beta f_1 f_4+\alpha\beta f_3 f_4)) \right) \\ -\frac{\alpha b\beta(f_3-f_4)}{\alpha f_4+\beta f_3-\beta f_4} \\ 0 \end{pmatrix}$$

and

$$Z = \begin{pmatrix} 0 & 0 \\ 0 & 0 \\ -\frac{b(\alpha f_4+\beta f_3-\beta f_4)}{\beta c} & 0 \\ 0 & \frac{b f_4(2\alpha-1)}{\beta c} \\ 0 & 0 \\ -\frac{\alpha b f_4}{\alpha f_4+\beta f_3-\beta f_4} & \frac{b(2\alpha-1)}{\alpha} \\ -\frac{b\beta(f_3-f_4)}{\alpha f_4+\beta f_3-\beta f_4} & 0 \\ 0 & -\frac{b(3\alpha-1)}{\alpha} \end{pmatrix}.$$

As mentioned above, this is a rather unique fixed point. It takes also lengthier computations to prove its stability. Recall the conditions for stability of this system, i.e. $\frac{1}{3} < \alpha < \frac{1}{2}, f_1 > f_4, f_3 > f_4$, and $f_4 > \beta f_2$.

We will verify the stability of this fixed point by analyzing the eigenvalues of this system. With the parameters $f_1 = 1.7$, $f_2 = 1$, $f_3 = 2$, $f_4 = 1.5$, $c = 1$, $p = 1$, $\alpha = 2/5$, $\beta = 4/25$, $b = 1$ that satisfy these conditions, the eigenvalues of the system at this fixed point are:

$$\lambda_1 = -8.3750 \qquad \lambda_2 = -0.5000$$
$$\lambda_3 = -0.0080 - 0.2187i \qquad \lambda_4 = -0.0080 + 0.2187i$$
$$\lambda_5 = -0.0469 - 0.5887i \qquad \lambda_6 = -0.0469 + 0.5887i$$
$$\lambda_7 = -0.4956 - 1.2448i \qquad \lambda_8 = -0.4956 + 1.2448i$$

Hence we can generate a system with the CRN in Fig. 4(b) which has a stable and robust steady state of LI.

A.3. Computations for minimal networks with a newly added viral variant connected to pre-existing persistent variants

In Section 3.1, we noted that the newly emerging variant has to elicit immune response against the pre-existing altruistic variant to maintain stable LI. Here we show the results of computations for cases when the newly emerged variant is connected to either of the two other persistent variants.

When the newly emerged variant is connected to the variant 1, the dynamics (1) of this CRN is described by the following equations

$$\begin{aligned} \dot{x}_1 &= f_1 x_1 - p x_1(r_1+\beta r_2), \\ \dot{x}_2 &= f_2 x2 - p x_2(r_2+\beta r_3), \\ \dot{x}_3 &= f_3 x_3 - p x_3(r_3+\beta r_2), \\ \dot{x}_4 &= f_4 x_4 - p x_4(r_4+\beta r_1), \\ \dot{r}_1 &= c\left(\frac{x_1 r_1}{r_1+\alpha r_2}+\frac{\alpha x_4 r_1}{\alpha r_1+r_4}\right) - b r_1, \\ \dot{r}_2 &= c\left(\frac{\alpha x_1 r_2}{r_1+\alpha r_2}+\frac{x_2 r_2}{r_2+\alpha r_3}+\frac{\alpha x_3 r_2}{r_3+\alpha r_2}\right) - b r_2, \\ \dot{r}_3 &= c\left(\frac{\alpha x_2 r_3}{r_2+\alpha r_3}+\frac{x_3 r_3}{r_3+\alpha r_2}\right) - b r_3, \\ \dot{r}_4 &= c\left(\frac{x_4 r_4}{r_4+\alpha r_1}\right) - b r_4. \end{aligned} \tag{A.3}$$

In the fixed point shown in Fig. A.7, the newly emergent variant becomes transient, and the resulting network is functionally the same as the branch-cycle network (Fig. 1). There is no transformation of functions in this case.

Fig. A.8 shows the fixed point

$$x_1 = \frac{b f_1(1-\alpha)}{\beta c p}, \quad x_2 = 0, \quad x_3 = \frac{b(\beta f_3+(\alpha-\beta)f_1)}{\beta c p}, \quad x_4 = \frac{b f_4}{c p}$$
$$r_1 = 0, \quad r_2 = \frac{f_1}{\beta p}, \quad r_3 = \frac{f_3-f_1}{p}, \quad r_4 = \frac{f_4}{p}$$

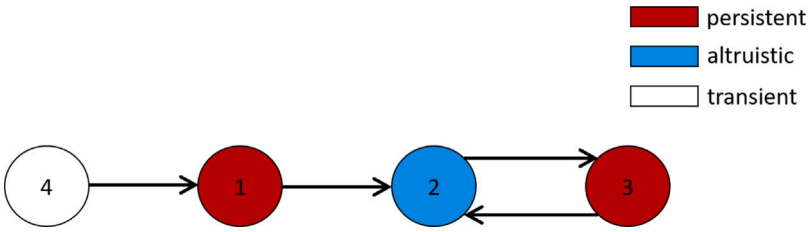

Fig. A.7. A fixed point when the newly emerging variant is connected to the variant 1 and becomes transient.

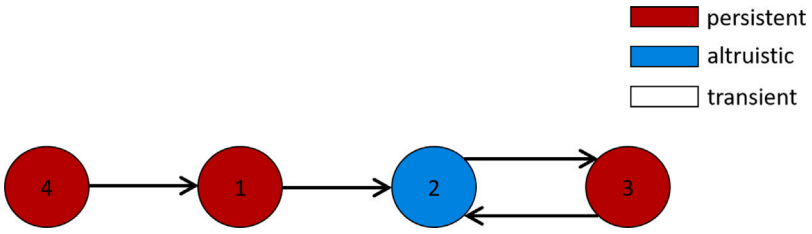

Fig. A.8. A fixed point when the newly emerging variant is connected to the variant 1 and becomes persistent.

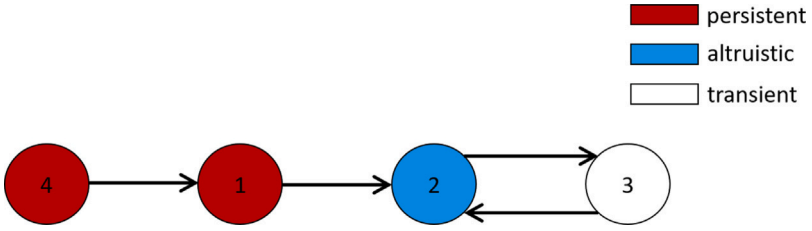

Fig. A.9. A fixed point when the newly emerging variant is connected to the variant 1 and becomes persistent, making the variant 3 transient.

The Jacobian at this fixed point is

$$\begin{pmatrix}
0 & 0 & 0 & 0 & \frac{bf_1(\alpha-1)}{\beta c} & \frac{bf_1(\alpha-1)}{c} & 0 & 0 \\
0 & -\frac{1}{\beta}(f_1-\beta f_2-\beta^2 f_1+\beta^2 f_3) & 0 & 0 & 0 & 0 & 0 & 0 \\
0 & 0 & 0 & 0 & 0 & -\frac{b}{c}(\alpha f_1-\beta f_1+\beta f_3) & -\frac{b((\alpha-\beta)f_1+\beta f_3)}{\beta c} & 0 \\
0 & 0 & 0 & 0 & -\frac{b\beta f_4}{c} & 0 & 0 & -\frac{bf_4}{c} \\
0 & 0 & 0 & 0 & \frac{b}{\alpha}(1-\alpha)^2 & 0 & 0 & 0 \\
c & \frac{cf_1}{f_1-\alpha\beta f_1+\alpha\beta f_3} & \frac{\alpha cf_1}{(\alpha-\beta)f_1+\beta f_3} & 0 & b(1-\frac{1}{\alpha}) & \frac{-b((\alpha-\beta)f_1+\beta f_3+\alpha\beta(f_1-f_3))}{(\alpha-\beta)f_1+\beta f_3} & -\frac{\alpha bf_1}{(\alpha-\beta)f_1+\beta f_3} & 0 \\
0 & \frac{\alpha\beta c(f_3-f_1)}{f_1-\alpha\beta f_1+\alpha\beta f_3} & \frac{\beta c(f_3-f_1)}{(\alpha-\beta)f_1+\beta f_3} & 0 & 0 & \frac{\alpha\beta b(f_1-f_3)}{(\alpha-\beta)f_1+\beta f_3} & \frac{b\beta(f_1-f_3)}{(\alpha-\beta)f_1+\beta f_3} & 0 \\
0 & 0 & 0 & c & -\alpha b & 0 & 0 & -b
\end{pmatrix}$$

This fixed point can exist under the conditions $\alpha < 1, f_1 < \frac{\beta f_3}{\beta-\alpha}$, and $f_3 > f_1$.

Analyzing the eigenvalues of the system at this point, we get $\lambda_3 = b(\alpha + \frac{1}{\alpha} - 2) > 0$. As at least one of the eigenvalues are positive, the fixed point is unstable. Other fixed points where virus 4 becomes persistent can be similarly proven to have unstable LI.

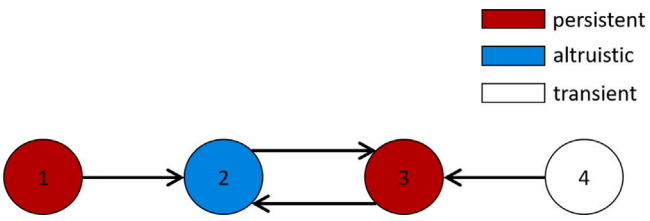

Fig. A.10. A fixed point when the newly emerging variant is connected to the variant 3 and becomes inactive.

The fixed points resulting in the network in Fig. A.9 are

$$x_1 = \frac{bf_1}{\beta cp}, \quad x_2 = 0, \quad x_3 = 0, \quad x_4 = \frac{bf_4}{cp}$$
$$r_1 = 0, \quad r_2 = \frac{f_1}{\beta p}, \quad r_3 = 0, \quad r_4 = \frac{f_4}{p}$$

The Jacobian at this fixed point is

$$\begin{pmatrix} 0 & 0 & 0 & 0 & -\frac{bf_1}{\beta c} & -\frac{bf_1}{c} & 0 & 0 \\ 0 & f_2 - \frac{f_1}{\beta} & 0 & 0 & 0 & 0 & 0 & 0 \\ 0 & 0 & f_3 - f_1 & 0 & 0 & 0 & 0 & 0 \\ 0 & 0 & 0 & 0 & -\frac{b\beta f_4}{c} & 0 & 0 & -\frac{bf_4}{c} \\ 0 & 0 & 0 & 0 & b(\alpha + \frac{1}{\alpha} - 1) & 0 & 0 & 0 \\ c & c & c & 0 & -\frac{b}{\alpha} & -b & 0 & 0 \\ 0 & 0 & 0 & 0 & 0 & 0 & -b & 0 \\ 0 & 0 & 0 & c & -\alpha b & 0 & 0 & -b \end{pmatrix}$$

Analyzing the eigenvalues of the system at this point, we get $\lambda_5 = b(\alpha + \frac{1}{\alpha} - 1) > 0$. As at least one of the eigenvalues are positive, the fixed point is unstable. Other fixed points where virus 4 becomes persistent can be similarly proven to have unstable LI.

Similarly, all networks where virus 4 is connected to virus 1 in the branch-cycle network can be shown to have either no LI or no stable LI.

Now we look at cases where the newly emerged variant is connected to the variant 3. The dynamics (1) of this population is described by the following equations

$$\begin{aligned} \dot{x}_1 &= f_1 x_1 - p x_1 (r_1 + \beta r_2), \\ \dot{x}_2 &= f_2 x2 - p x_2 (r_2 + \beta r_3), \\ \dot{x}_3 &= f_3 x_3 - p x_3 (r_3 + \beta r_2), \\ \dot{x}_4 &= f_4 x_4 - p x_4 (r_4 + \beta r_3), \\ \dot{r}_1 &= c(\frac{x_1 r_1}{r_1 + \alpha r_2}) - b r_1, \\ \dot{r}_2 &= c(\frac{\alpha x_1 r_2}{r_1 + \alpha r_2} + \frac{x_2 r_2}{r_2 + \alpha r_3} + \frac{\alpha x_3 r_2}{r_3 + \alpha r_2}) - b r_2, \\ \dot{r}_3 &= c(\frac{\alpha x_2 r_3}{r_2 + \alpha r_3} + \frac{x_3 r_3}{r_3 + \alpha r_2} + + \frac{\alpha x_4 r_3}{r_4 + \alpha r_3}) - b r_3, \\ \dot{r}_4 &= c(\frac{x_4 r_4}{r_4 + \alpha r_3}) - b r_4. \end{aligned} \tag{A.4}$$

The stable network obtained from this network is shown in Fig. A.10.

The fixed points resulting in the network in Fig. A.10 are

$$x_1 = \frac{bf_1}{\beta cp}(1 - \alpha), \quad x_2 = 0, \quad x_3 = \frac{b}{\beta cp}((\alpha - \beta) f_1 + \beta f_3), \quad x_4 = 0$$
$$r_1 = 0, \quad r_2 = \frac{f_1}{\beta p}, \quad r_3 = \frac{f_3 - f_1}{p}, \quad r_4 = 0$$

This network A.10 has the newly emerged variant being transient, and the resulting network is the same as the initial branch-cycle network.

A.4. Computations for merging of two minimal networks

Fig. 5 depicts three instances where two symmetric minimal networks are connected to each other to form three different types of networks. The dynamics (1) of this configuration is as follows:

$$
\begin{aligned}
\dot{x}_1 &= f_1 x_1 - p x_1 (r_1 + \beta r_2 + \beta r_5),\\
\dot{x}_2 &= f_2 x2 - p x_2 r_2,\\
\dot{x}_3 &= f_3 x_3 - p x_3 (r_3 + \beta r_2),\\
\dot{x}_4 &= f_4 x_4 - p x_4 (r_4 + \beta r_2 + \beta r_5),\\
\dot{x}_5 &= f_5 x_5 - p x_5 r_5,\\
\dot{x}_6 &= f_6 x_6 - p x_6 (r_6 + \beta r_5),\\
\dot{r}_1 &= c\left(\frac{x_1 r_1}{r_1 + \alpha r_2 + \alpha r_5}\right) - b r_1,\\
\dot{r}_2 &= c\left(\frac{\alpha x_1 r_2}{r_1 + \alpha r_2 + \alpha r_5} + x_2 + \frac{\alpha x_3 r_2}{r_3 + \alpha r_2} + \frac{\alpha x_4 r_2}{r_4 + \alpha r_2 + \alpha r_5}\right) - b r_2,\\
\dot{r}_3 &= c\left(\frac{x_3 r_3}{r_3 + \alpha r_2}\right) - b r_3,\\
\dot{r}_4 &= c\left(\frac{x_4 r_4}{r_4 + \alpha r_2 + \alpha r_5}\right) - b r_4,\\
\dot{r}_5 &= c\left(\frac{\alpha x_1 r_5}{r_1 + \alpha r_2 + \alpha r_5} + \frac{\alpha x_4 r_5}{r_4 + \alpha r_2 + \alpha r_5} + x_5 + \frac{\alpha x_6 r_5}{r_6 + \alpha r_5}\right) - b r_5,\\
\dot{r}_6 &= c\left(\frac{x_6 r_6}{r_6 + \alpha r_5}\right) - b r_6.
\end{aligned}
\tag{A.5}
$$

The Jacobian of the system of Eqs. (A.5) at the fixed point shown in Fig. 5(a) equals:

$$J = \begin{pmatrix} X & Y \end{pmatrix}$$

where

$$
X = \begin{pmatrix}
f_1 - f_4 & 0 & 0 & 0 & 0 & 0 & 0\\
0 & f_2 - \frac{f_4}{\beta} & 0 & 0 & 0 & 0 & 0\\
0 & 0 & 0 & 0 & 0 & 0 & 0\\
0 & 0 & 0 & 0 & 0 & 0 & 0\\
0 & 0 & 0 & 0 & f_5 & 0 & 0\\
0 & 0 & 0 & 0 & 0 & 0 & 0\\
0 & 0 & 0 & 0 & 0 & 0 & -b\\
c & c & \frac{\alpha c f_4}{\alpha f_4 + \beta f_3 - \beta f_4} & c & 0 & 0 & 0\\
0 & 0 & \frac{\beta c (f_3 - f_4)}{\alpha f_4 + \beta f_3 - \beta f_4} & 0 & 0 & 0 & 0\\
0 & 0 & 0 & 0 & 0 & 0 & 0\\
0 & 0 & 0 & 0 & c & 0 & 0\\
0 & 0 & 0 & 0 & 0 & c & 0
\end{pmatrix},
$$

and

$$
Y = \begin{pmatrix}
0 & 0 & 0 & 0 & 0\\
0 & 0 & 0 & 0 & 0\\
-\frac{b(\alpha f_4 + \beta f_3 - \beta f_4)}{c} & -\frac{b(\alpha f_4 + \beta f_3 - \beta f_4)}{\beta c} & 0 & 0 & 0\\
\frac{b f_4 (\alpha - 1)}{c} & 0 & \frac{b f_4 (\alpha - 1)}{\beta c} & \frac{b f_4 (\alpha - 1)}{c} & 0\\
0 & 0 & 0 & 0 & 0\\
0 & 0 & 0 & -\frac{b \beta f_6}{c} & -\frac{b f_6}{c}\\
0 & 0 & 0 & 0 & 0\\
-\frac{b(\alpha f_4 + \beta f_3 - \beta f_4 - \alpha \beta f_3 + \alpha \beta f_4)}{\alpha f_4 + \beta f_3 - \beta f_4} & -\frac{\alpha b f_4}{\alpha f_4 + \beta f_3 - \beta f_4} & \frac{b(\alpha - 1)}{\alpha} & b(\alpha - 1) & 0\\
-\frac{\alpha b \beta (f_3 - f_4)}{\alpha f_4 + \beta f_3 - \beta f_4} & -\frac{b \beta (f_3 - f_4)}{\alpha f_4 + \beta f_3 - \beta f_4} & 0 & 0 & 0\\
0 & 0 & -\frac{b(2\alpha - 1)}{\alpha} & 0 & 0\\
0 & 0 & 0 & 0 & 0\\
0 & 0 & 0 & -\alpha b & -b
\end{pmatrix}.
$$

We will verify the stability of this fixed point by analyzing the eigenvalues of this system. With the parameters $f_1 = 0.25$, $f_2 = 0.3$, $f_3 = 0.35$, $f_4 = 0.3$, $f_5 = 0.35$, $f_6 = 0.4$, $c = 1$, $p = 2$, $\alpha = 1/3$, $\beta = 1/9$, $b = 3$ that satisfy the conditions for our fixed point, the eigenvalues of the system at this fixed point are:

$\lambda_1 = -0.0500$ $\lambda_2 = 0.0000$

$\lambda_3 = 0.0000$ $\lambda_4 = 0.0000$

$\lambda_5 = 0.0000$ $\lambda_6 = 0.0000$

$\lambda_7 = -2.5247$ $\lambda_8 = -0.4753$

$\lambda_9 = -2.6396$ $\lambda_{10} = -0.3525$

$\lambda_{11} = -0.0566 - 0.3058i$ $\lambda_{12} = -0.0566 + 0.3058i$

The Jacobian of the fixed point in Fig. 5(b) is $J = (W\,X\,Y\,Z)$ where

$$W = \begin{pmatrix} f_1 - f_4 & 0 & 0 & 0 & 0 \\ 0 & f_2 - \frac{f_4 - \beta f_5}{\beta} & 0 & 0 & 0 \\ 0 & 0 & 0 & 0 & 0 \\ 0 & 0 & 0 & 0 & 0 \\ 0 & 0 & 0 & 0 & 0 \\ 0 & 0 & 0 & 0 & 0 \\ 0 & 0 & 0 & 0 & 0 \\ \frac{c(f_4 - \beta f_5)}{f_4} & c & \frac{\alpha c(f_4 - \beta f_5)}{\alpha f_4 + \beta f_3 - \beta f_4 + \beta^2 f_5 - \alpha\beta f_5} & \frac{c(f_4 - \beta f_5)}{f_4} & 0 \\ 0 & 0 & \frac{\beta c(f_3 - f_4 + \beta f_5)}{\alpha f_4 + \beta f_3 - \beta f_4 + \beta^2 f_5 - \alpha\beta f_5} & 0 & 0 \\ 0 & 0 & 0 & 0 & 0 \\ \frac{\beta c f_5}{f_4} & 0 & 0 & \frac{\beta c f_5}{f_4} & c \\ 0 & 0 & 0 & 0 & 0 \end{pmatrix},$$

$$X = \begin{pmatrix} 0 & 0 & 0 \\ 0 & 0 & 0 \\ 0 & 0 & -\frac{b(\alpha f_4 + \beta f_3 - \beta f_4 + \beta^2 f_5 - \alpha\beta f_5)}{c} \\ 0 & 0 & \frac{b f_4(\alpha - 1)}{c} \\ 0 & 0 & 0 \\ 0 & 0 & 0 \\ 0 & -b & 0 \\ 0 & 0 & -\frac{b(f_4 - \beta f_5)(\alpha f_4 + \beta f_3 - \beta f_4 + \beta^2 f_5 - \alpha\beta f_3 + \alpha\beta f_4 - \alpha\beta f_5 - \alpha\beta^2 f_5 + \alpha^2\beta f_5)}{f_4(\alpha f_4 + \beta f_3 - \beta f_4 + \beta^2 f_5 - \alpha\beta f_5)} \\ 0 & 0 & -\frac{\alpha b\beta(f_3 - f_4 + \beta f_5)}{\alpha f_4 + \beta f_3 - \beta f_4 + \beta^2 f_5 - \alpha\beta f_5} \\ 0 & 0 & 0 \\ \frac{\alpha c f_5}{f_6 + \alpha f_5 - \beta f_5} & 0 & \frac{b\beta f_5(\alpha - 1)}{f_4} \\ \frac{c(f_6 - \beta f_5)}{f_6 + \alpha f_5 - \beta f_5} & 0 & 0 \end{pmatrix},$$

$$Y = \begin{pmatrix} 0 & 0 \\ 0 & 0 \\ -\frac{b(\alpha f_4 + \beta f_3 - \beta f_4 + \beta^2 f_5 - \alpha\beta f_5)}{\beta c} & 0 \\ 0 & \frac{b f_4(\alpha - 1)}{\beta c} \\ 0 & 0 \\ 0 & 0 \\ 0 & 0 \\ -\frac{\alpha b(f_4 - \beta f_5)}{\alpha f_4 + \beta f_3 - \beta f_4 + \beta^2 f_5 - \alpha\beta f_5} & \frac{b(\alpha - 1)(f_4 - \beta f_5)}{\alpha f_4} \\ -\frac{b\beta(f_3 - f_4 + \beta f_5)}{\alpha f_4 + \beta f_3 - \beta f_4 + \beta^2 f_5 - \alpha\beta f_5} & 0 \\ 0 & -\frac{b(2\alpha - 1)}{\alpha} \\ 0 & \frac{b\beta f_5(\alpha - 1)}{\alpha f_4} \\ 0 & 0 \end{pmatrix},$$

and

$$Z = \begin{pmatrix} 0 & 0 \\ 0 & 0 \\ 0 & 0 \\ \frac{b f_4(\alpha - 1)}{c} & 0 \\ 0 & 0 \\ -\frac{b\beta(f_6 + \alpha f_5 - \beta f_5)}{c} & -\frac{b(f_6 + \alpha f_5 - \beta f_5)}{c} \\ 0 & 0 \\ \frac{b(\alpha - 1)(f_4 - \beta f_5)}{f_4} & 0 \\ 0 & 0 \\ 0 & 0 \\ -\frac{b f_5(\beta f_6 + \alpha^2 f_4 - \beta^2 f_5 + \alpha\beta f_5 - \alpha\beta f_6 + \alpha\beta^2 f_5 - \alpha^2\beta f_5)}{f_4(f_6 + \alpha f_5 - \beta f_5)} & -\frac{\alpha b f_5}{f_6 + \alpha f_5 - \beta f_5} \\ -\frac{\alpha b(f_6 - \beta f_5)}{f_6 + \alpha f_5 - \beta f_5} & -\frac{b(f_6 - \beta f_5)}{f_6 + \alpha f_5 - \beta f_5} \end{pmatrix}.$$

We will present an exact example with the stable state of local immunodeficiency. Let the system's parameters have the following values $f_1 = 0.25, f_2 = 0.3, f_3 = 0.35, f_4 = 0.3, f_5 = 0.35, f_6 = 0.4, c = 1, p = 2, \alpha = 1/3, \beta = 1/9, b = 3$. One can compute the corresponding Jacobian numerically and confirm that all the eigenvalues are either real negative or complex with negative real parts. It follows by continuity that there exists a positive measure set in the parameter space such that for any point (a set of parameters) the corresponding state of local immunodeficiency is stable.

Finally, the Jacobian computed at the fixed point shown in Fig. 5(c) is $J = XY$ where

$$X = \begin{pmatrix} f_1 - f_6 - \beta f_2 & 0 & 0 & 0 & 0 & 0 \\ 0 & 0 & 0 & 0 & 0 & 0 \\ 0 & 0 & 0 & 0 & 0 & 0 \\ 0 & 0 & 0 & f_4 - f_6 - \beta f_2 & 0 & 0 \\ 0 & 0 & 0 & 0 & f_5 - \frac{f_6}{\beta} & 0 \\ 0 & 0 & 0 & 0 & 0 & 0 \\ 0 & 0 & 0 & 0 & 0 & 0 \\ \frac{\beta c f_2}{f_6+\beta f_2} & c & \frac{\alpha c f_2}{f_3+\alpha f_2-\beta f_2} & \frac{\beta c f_2}{f_6+\beta f_2} & 0 & 0 \\ 0 & 0 & \frac{c(f_3-\beta f_2)}{f_3+\alpha f_2-\beta f_2} & 0 & 0 & 0 \\ 0 & 0 & 0 & 0 & 0 & 0 \\ \frac{c f_6}{f_6+\beta f_2} & 0 & 0 & \frac{c f_6}{f_6+\beta f_2} & c & c \\ 0 & 0 & 0 & 0 & 0 & 0 \end{pmatrix},$$

$$Y = \begin{pmatrix} 0 & 0 & 0 & 0 & 0 & 0 \\ 0 & \frac{b f_2 (\alpha-1)}{c} & 0 & 0 & 0 & 0 \\ 0 & -\frac{b\beta(f_3+\alpha f_2-\beta f_2)}{c} & -\frac{b(f_3+\alpha f_2-\beta f_2)}{c} & 0 & 0 & 0 \\ 0 & 0 & 0 & 0 & 0 & 0 \\ 0 & 0 & 0 & 0 & 0 & 0 \\ 0 & 0 & 0 & 0 & -\frac{b f_6}{c} & -\frac{b f_6}{\beta c} \\ -b & 0 & 0 & 0 & 0 & 0 \\ 0 & -\frac{b(f_3+\alpha f_2-\alpha f_3-\beta f_2+\alpha\beta f_2)}{f_3+\alpha f_2-\beta f_2} & -\frac{\alpha b f_2}{f_3+\alpha f_2-\beta f_2} & 0 & 0 & 0 \\ 0 & -\frac{\alpha b(f_3-\beta f_2)}{f_3+\alpha f_2-\beta f_2} & -\frac{b(f_3-\beta f_2)}{f_3+\alpha f_2-\beta f_2} & 0 & 0 & 0 \\ 0 & 0 & 0 & -b & 0 & 0 \\ 0 & 0 & 0 & 0 & -b & -\frac{b}{\alpha} \\ 0 & 0 & 0 & 0 & 0 & -\frac{b(\alpha-1)}{\alpha} \end{pmatrix},$$

In this case also, we present an exact numerical example with a stable state of local immunodeficiency. Let the system's parameters assume the following values $f_1 = 0.25, f_2 = 0.3, f_3 = 0.35, f_4 = 0.3, f_5 = 0.35, f_6 = 0.4, c = 1, p = 2, \alpha = 1/3, \beta = 1/9, b = 3$. One can compute the corresponding Jacobian numerically and confirm that all the eigenvalues are either real negative or complex with negative real parts. Once again, it follows by continuity that there exists a positive measure set in the parameter space where the state of a local immunodeficiency is stable.

References

Baykal, P.B.I., Lara, J., Khudyakov, Y., Zelikovsky, A., Skums, P., 2021. Quantitative differences between intra-host HCV populations from persons with recently established and persistent infections. Virus Evol. 6 (2), veaa103.

Bunimovich, L., Shu, L., 2019. Local immunodeficiency: Minimal networks and stability. Math. Biosci. 310, 31–49. http://dx.doi.org/10.1016/j.mbs.2019.02.002, URL https://www.sciencedirect.com/science/article/pii/S002555641830498X.

Bunimovich, L., Shu, L., 2020. Local immunodeficiency: Role of neutral viruses. Bull. Math. Biol. 82, http://dx.doi.org/10.1007/s11538-020-00813-z, URL https://link.springer.com/article/10.1007/s11538-020-00813-z.

Bunimovich, L., Smith, D., Webb, B.Z., 2019. Specialization models of network growth. J. Complex Netw. 7 (3), 375–392.

Campo, D.S., Dimitrova, Z., Yamasaki, L., Skums, P., Lau, D., Vaughan, G., Forbi, J., Teo, C.-G., Khudyakov, Y., 2014. Next-generation sequencing reveals large connected networks of intra-host HCV variants. BMC Genomics 15 (Suppl 5), S4. http://dx.doi.org/10.1186/1471-2164-15-S5-S4, URL http://www.biomedcentral.com/1471-2164/15/S5/S4.

Campo, D.S., Dimitrova, Z., Yokosawa, J., Hoang, D., Perez, N.O., Ramachandran, S., Khudyakov, Y., 2012. Hepatitis C virus antigenic convergence. Sci. Rep. 2, 267.

Campo, D.S., Zhang, J., Ramachandran, S., Khudyakov, Y., 2017. Transmissibility of intra-host hepatitis C virus variants. BMC Genomics 18 (10), 11–19.

Domingo, E., Sheldon, J., Perales, C., 2012. Viral quasispecies evolution. Microbiol. Mol. Biol. Rev. 76 (2), 159–216.

Domingo-Calap, P., Segredo-Otero, E., Durán-Moreno, M., Sanjuán, R., 2019. Social evolution of innate immunity evasion in a virus. Nat. Microbiol. 1.

Drake, J.W., Holland, J.J., 1999. Mutation rates among RNA viruses. Proc. Natl. Acad. Sci. 96 (24), 13910–13913.

Francis, T., 1960. On the doctrine of original antigenic sin. Proc. Am. Phil. Soc. 104 (6), 572–578.

Freitas, A.A., Rosado, M.M., Viale, A.-C., Grandien, A., 1995. The role of cellular competition in B cell survival and selection of B cell repertoires. Euro. J. Immunol. 25 (6), 1729–1738.

Gismondi, M.I., Carrasco, J.M.D., Valva, P., Becker, P.D., Guzmán, C.A., Campos, R.H., Preciado, M.V., 2013. Dynamic changes in viral population structure and compartmentalization during chronic hepatitis C virus infection in children. Virology 447 (1), 187–196.

Gog, J.R., Grenfell, B.T., 2002. Dynamics and selection of many-strain pathogens. Proc. Natl. Acad. Sci. 99 (26), 17209–17214.

Gray, R.R., Salemi, M., Klenerman, P., Pybus, O.G., 2012. A new evolutionary model for hepatitis C virus chronic infection. PLoS Pathog. 8 (5), e1002656.

Hamilton, W.D., 1964. The genetical evolution of social behaviour. II. J. Theoret. Biol. 7 (1), 17–52.

Haraguchi, Y., Sasaki, A., 1997. Evolutionary pattern of intra–host pathogen antigenic drift: effect of cross–reactivity in immune response. Philos. Trans. R. Soc. London Ser. B: Biol. Sci. 352 (1349), 11–20.

Illingworth, C.J., Fischer, A., Mustonen, V., 2014. Identifying selection in the within-host evolution of influenza using viral sequence data. PLoS Comput. Biol. 10 (7), e1003755.

Iwasa, Y., Michor, F., Nowak, M., 2004. Some basic properties of immune selection. J. Theoret. Biol. 229 (2), 179–188.

Kim, J.H., Skountzou, I., Compans, R., Jacob, J., 2009. Original antigenic sin responses to influenza viruses. J. Immunol. 183 (5), 3294–3301.

Lu, L., Tatsunori, N., Li, C., Waheed, S., Gao, F., Robertson, B.H., 2008. HCV selection and HVR1 evolution in a chimpanzee chronically infected with HCV-1 over 12 years. Hepatol. Res. 38 (7), 704–716.

McLean, A., Rosado, M., Agenes, F., Vasconcellos, R., Freitas, A.A., 1997. Resource competition as a mechanism for B cell homeostasis. Proc. Natl. Acad. Sci. 94 (11), 5792–5797.

Meyer, K., Ait-Goughoulte, M., Keck, Z.-Y., Foung, S., Ray, R., 2008. Antibody-dependent enhancement of hepatitis C virus infection. J. Virol. 82 (5), 2140–2149.

Midgley, C.M., Bajwa-Joseph, M., Vasanawathana, S., Limpitikul, W., Wills, B., Flanagan, A., Waiyaiya, E., Tran, H.B., Cowper, A.E., Chotiyarnwon, P., et al., 2011. An in-depth analysis of original antigenic sin in dengue virus infection. J. Virol. 85 (1), 410–421.

Nagot, N., Binh, N.T., Hong, T.T., Vinh, V.H., Quillet, C., Vallo, R., Huong, D.T., Oanh, K.T.H., Thanh, N.T.T., Rapoud, D., et al., 2023. A community-based strategy to eliminate hepatitis C among people who inject drugs in Vietnam. Lancet Reg. Health–West. Pac..

Nara, P.L., Tobin, G.J., Chaudhuri, A.R., Trujillo, J.D., Lin, G., Cho, M.W., Levin, S.A., Ndifon, W., Wingreen, N.S., 2010. How can vaccines against influenza and other viral diseases be made more effective? PLoS Biol. 8 (12), e1000571.

Nowak, M.A., Anderson, R.M., McLean, A.R., Wolfs, T.F., Goudsmit, J., May, R.M., 1991. Antigenic diversity thresholds and the development of AIDS. Science 254 (5034), 963–969. http://dx.doi.org/10.1126/science.1683006, URL https://www.ncbi.nlm.nih.gov/pubmed/1683006.

Nowak, M.A., May, R.M., 1991. Mathematical biology of HIV infections: antigenic variation and diversity threshold. Math. Biosci. 106 (1), 1–21. http://dx.doi.org/10.1016/0025-5564(91)90037-j, URL https://www.ncbi.nlm.nih.gov/pubmed/1802171.

Nowak, M.A., May, R.M., 2000. Virus Dynamics. Mathematical Principles of Immunology and Virology. Oxford University Press, Oxford.

Nowak, M.A., May, R.M., Anderson, R.M., 1990. The evolutionary dynamics of HIV-1 quasispecies and the development of immunodeficiency disease. AIDS 4 (11), 1095–1103. http://dx.doi.org/10.1097/00002030-199011000-00007, URL https://www.ncbi.nlm.nih.gov/pubmed/2282182.

Organization, W.H., et al., 2016. Combating Hepatitis B and C to Reach Elimination by 2030: Advocacy Brief. Tech. rep., World Health Organization.

Palmer, B.A., Dimitrova, Z., Skums, P., Crosbie, O., Kenny-Walsh, E., Fanning, L.J., 2014. Analysis of the evolution and structure of a complex intrahost viral population in chronic hepatitis C virus mapped by ultradeep pyrosequencing. J. Virol. 88 (23), 13709–13721.

Palmer, B.A., Moreau, I., Levis, J., Harty, C., Crosbie, O., Kenny-Walsh, E., Fanning, L.J., 2012. Insertion and recombination events at hypervariable region 1 over 9.6 years of hepatitis C virus chronic infection. J. Gen. Virol. 93 (12), 2614–2624.

Parsons, M.S., Muller, S., Kohler, H., Grant, M.D., Bernard, N.F., 2013. On the benefits of sin: can greater understanding of the 1f7-idiotypic repertoire freeze enhance HIV vaccine development? Hum. Vaccines Immunother. 9 (7), 1532–1538.

Raghwani, J., Rose, R., Sheridan, I., Lemey, P., Suchard, M.A., Santantonio, T., Farci, P., Klenerman, P., Pybus, O.G., 2016. Exceptional heterogeneity in viral evolutionary dynamics characterises chronic hepatitis C virus infection. PLoS Pathog. 12 (9), e1005894.

Ramachandran, S., Campo, D.S., Dimitrova, Z.E., Xia, G.-l., Purdy, M.A., Khudyakov, Y.E., 2011. Temporal variations in the hepatitis C virus intrahost population during chronic infection. J. Virol. 85 (13), 6369–6380.

Rehermann, B., Shin, E.-C., 2005. Private aspects of heterologous immunity. J. Exp. Med. 201 (5), 667–670.

Rhee, S.-Y., Liu, T., Holmes, S., Shafer, R., 2007. HIV-1 subtype B protease and reverse transcriptase amino acid covariation. PLoS Comput. Biol. 3, e87.

Schwickert, T.A., Lindquist, R.L., Shakhar, G., Livshits, G., Skokos, D., Kosco-Vilbois, M.H., Dustin, M.L., Nussenzweig, M.C., 2007. In vivo imaging of germinal centres reveals a dynamic open structure. Nature 446 (7131), 83–87.

Shirogane, Y., Watanabe, S., Yanagi, Y., 2013. Cooperation: another mechanism of viral evolution. Trends Microbiol. 21 (7), 320–324.

Skums, P., Bunimovich, L., Khudyakov, Y., 2015a. Antigenic cooperation among intrahost HCV variants organized into a complex network of cross-immunoreactivity. Proc. Natl. Acad. Sci. 112 (21), 6653–6658.

Skums, P., Glebova, O., Campo, D.S., Li, N., Dimitrova, Z., Sims, S., Bunimovich, L., Zelikovsky, A., Khudyakov, Y., 2015b. Algorithms for prediction of viral transmission using analysis of intra-host viral populations. In: Computational Advances in Bio and Medical Sciences (ICCABS), 2015 IEEE 5th International Conference on. IEEE, p. 1.

Tarlinton, D., 2006. B-cell memory: are subsets necessary? Nat. Rev. Immunol. 6 (10), 785–790.

Van Regenmortel, M.H., 2012. Basic research in HIV vaccinology is hampered by reductionist thinking. Front. Immunol. 3.

Wodarz, D., 2003. Hepatitis C virus dynamics and pathology: the role of CTL and antibody responses. J. Gen. Virol. 84 (Pt 7), 1743–1750. http://dx.doi.org/10.1099/vir.0.19118-0, URL https://www.ncbi.nlm.nih.gov/pubmed/12810868.